
Universiteit
Leiden
The Netherlands

Holding the balance; the equilibrium between ERα-activation, epigenetic alterations and chromatin integrity

Flach, K.D.

Citation
Flach, K. D. (2018, September 25). *Holding the balance; the equilibrium between ERα-activation, epigenetic alterations and chromatin integrity*. Retrieved from https://hdl.handle.net/1887/66110

Version:	Not Applicable (or Unknown)
License:	Licence agreement concerning inclusion of doctoral thesis in the Institutional Repository of the University of Leiden
Downloaded from:	https://hdl.handle.net/1887/66110

Note: To cite this publication please use the final published version (if applicable).

Cover Page

Universiteit Leiden

The handle http://hdl.handle.net/1887/66110 holds various files of this Leiden University dissertation.

Author: Flach, K.D.
Title: Holding the balance; the equilibrium between ERα-activation, epigenetic alterations and chromatin integrity
Issue Date: 2018-09-25

Chapter 3

Posttranslational modification of ERα -part 2

Interaction of 14-3-3 proteins with the estrogen receptor alpha F domain provides a drug target interface

Ingrid J. De Vries-van Leeuwen[a], Daniel da Costa Pereira[a], Koen D. Flach[b], Sander R. Piersma[c], Christian Haase[d], David Bier[e], Zeliha Yalcin[a], Rob Michalides[b], K. Anton Feenstra[f], Connie R. Jiménez[c], Tom F. A. de Greef[g], Luc Brunsveld[d], Christian Ottmann[d,e], Wilbert Zwart[b], and Albertus H. de Boer[a]

[a]Department of Structural Biology, Faculty Earth and Life Sciences, Vrije Universiteit, 1081 HV Amsterdam, The Netherlands
[b]Department of Molecular Pathology, Netherlands Cancer Institute, 1066 CX Amsterdam, The Netherlands
[c]OncoProteomics Laboratory, Department of Medical Oncology, VU University Medical Center, 1081 HV Amsterdam, The Netherlands
[d]Chemical Biology Laboratory, Department of Biomedical Engineering, Eindhoven University of Technology, 5612 AZ, Eindhoven, The Netherlands
[e]Chemical Genomics Centre, Max Planck Institute of Molecular Physiology, 44227 Dortmund, Germany
[f]Center for Integrative Bioinformatics, Vrije Universiteit, 1081 HV Amsterdam, The Netherlands
[g]Institute for Complex Molecular Systems, Eindhoven University of Technology, 5600 MB Eindhoven, The Netherlands

PNAS (2013) May 28;110(22):8894-9

Abstract
Estrogen receptor alpha (ERα) is involved in numerous physiological and pathological processes, including breast cancer. Breast cancer therapy is therefore currently directed at inhibiting the transcriptional potency of ERα, either by blocking estrogen production through aromatase inhibitors or anti-estrogens that compete for hormone binding. Due to resistance, new treatment modalities are needed and as ERα dimerization is essential for its activity, interference with receptor dimerization offers a new opportunity to exploit in drug design. Here we describe a unique mechanism of how ERα dimerization is negatively controlled by interaction with 14-3-3 proteins at the extreme C terminus of the receptor. Moreover, the small-molecule fusicoccin (FC) stabilizes this ERα/14-3-3 interaction. Cocrystallization of the trimeric ERα/14-3-3/FC complex provides the structural basis for this stabilization and shows the importance of phosphorylation of the penultimate Threonine (ERα-T594) for high-affinity interaction. We confirm that T594 is a distinct ERα phosphorylation site in the breast cancer cell line MCF-7 using a phospho-T594–specific antibody and by mass spectrometry. In line with its ERα/14-3-3 interaction stabilizing effect, fusicoccin reduces the estradiol-stimulated ERα dimerization, inhibits ERα/chromatin interactions and downstream gene expression, resulting in decreased cell proliferation. Herewith, a unique functional phosphosite and an alternative regulation mechanism of ERα are provided, together with a small molecule that selectively targets this ERα/14-3-3 interface.

Introduction

The estrogen receptor alpha (ERα) is a ligand-dependent transcription factor and the driving force of cell proliferation in 75% of all breast cancers. Current therapeutic strategies to treat these tumors rely on selective ER modulators (SERMs), like tamoxifen (TAM) (1) or aromatase inhibitors (AIs) that block estradiol synthesis (2). Although the benefits of treating hormone-sensitive breast cancers with SERMs and AIs are evident, resistance to treatment is commonly observed (3, 4). To overcome resistance, selective ERα down-regulators (SERDs) can for instance be applied that inhibit ERα signaling through receptor degradation (5, 6). Approaches that target the ERα/DNA or ERα/co-factor interactions are explored as well (5, 7), but other essential steps in the ERα activation cascade are currently unexploited in drug design, also due to a lack of molecular understanding of the processes at hand.

One such step that is crucial for many aspects of ERα functioning is ligand-driven receptor dimerization (8, 9). 17β-Estradiol (E2) association with the ERα ligand binding domain (LBD) drives large conformational changes (10) resulting in ERα dissociation from chaperones (11, 12), unmasking of domains for receptor dimerization, and DNA binding (13, 14). Whereas the LBD contains the main dimerization domain (15), the extreme C-terminal domain of the receptor (F domain) imposes a restraint on dimerization (15, 16), although the regulation of this remains fully elusive. The F domain is a relatively understudied part of the receptor and due to its flexibility, no structural information has been available until now (16). Analysis of F-domain truncation mutants point to an important role for the last few amino acids in receptor dimerization and transactivation activity (17).

Recently, we reported that the diterpene glucoside fusicoccin (FC), a product of the fungus Phomopsis amygdali (18), induces apoptosis in a number of cancer cell lines, in synergy with the cytokine IFN alpha (IFNα) (19). In plants, the molecular mechanism of FC's action is highly specific through a unique stabilization of the interaction of 14-3-3 proteins and the C terminus of plasma membrane proton ATPases, with a key role for the penultimate (phosphorylated) Thr of the ATPase (20–22). 14-3-3 Proteins are a family of adapter proteins conserved in all eukaryotic organisms, with key positions in vital cellular processes as well as pathogenesis, like neurodegeneration and tumor development (23, 24). The sequence homology of the extreme C terminus of the plant ATPase and human ERα and the observed effect of FC on the growth of ERα positive breast tumor cells led us to explore the effect of FC on ERα function in these cells.

We show here that ERα interacts with 14-3-3 proteins, with a key role for the penultimate Threonine of ERα (T594). Mutation of T594 strongly enhances the estradiol-dependent ERα dimerization and transactivation. As shown by cocrystallization, binding of the T594 phosphorylated ERα C terminus in the 14-3-3 binding groove leaves a cavity that can be filled by the FC molecule. We confirm that T594 is a distinct ERα phosphorylation site in the breast cancer cell line MCF-7 using a phospho-T594–specific antibody and by mass spectrometry. Furthermore, FC has a negative effect on ERα/chromatin interactions, E2-dependent gene transcription, and cell growth. With this, we provide an alternative ERα regulating mechanism, involving the ERα F domain and provide a unique druggable interface between ERα and 14-3-3 proteins, together with a small molecule (FC) that functions as a proof of principle, which highlights the potential druggability of this protein/protein interaction surface for alternative therapeutics design in breast cancer.

Results

ERα F Domain Interacts with 14-3-3 Proteins.

Sequence alignment of the ERα F domain from a wide range of animals, from human to frog, shows a high degree of variation in amino acid composition, with the exception of the last two amino acids, which are invariably Thr,Val or Thr,Ile (TV or TI) (**Fig. 1A**). This conservation of the ERα C terminus points to a conserved function of the tip and in view of the analogy with the plant ATPase C-terminal tip (Fig. S1A), which is involved in 14-3-3 interactions (22, 25), we performed a yeast-two hybrid (Y2H) assay with the C-terminal half of ERα (ERα-LBD302–595) against all seven human 14-3-3 isoforms. Yeast growth is observed with all 14-3-3 isoforms on triple drop-out plates (**Fig. 1B**), providing evidence for direct physical interaction between these proteins. The penultimate T594 of ERα is essential for 14-3-3 interaction because cells transformed with ERαT594A did not grow (**Fig. 1B**). Helix 12, which is directly N terminal to the F domain, undergoes dramatic conformational changes upon ligand binding (26) and this will most likely change the position of the F domain as well. To test whether ligand binding renders the F domain more accessible for interaction with 14-3-3 proteins, a yeast two-hybrid (β-galactosidase, β-gal) assay was performed to quantitatively assess the ERα/14-3-3 interaction. Both E2 and 4-hydroxytamoxifen (4OH-TAM) strongly enhance the ERα-LBD/14-3-3θ interaction and again ERα-LBDT594A does not interact with 14-3-3θ (**Fig. 1C**). Similar results

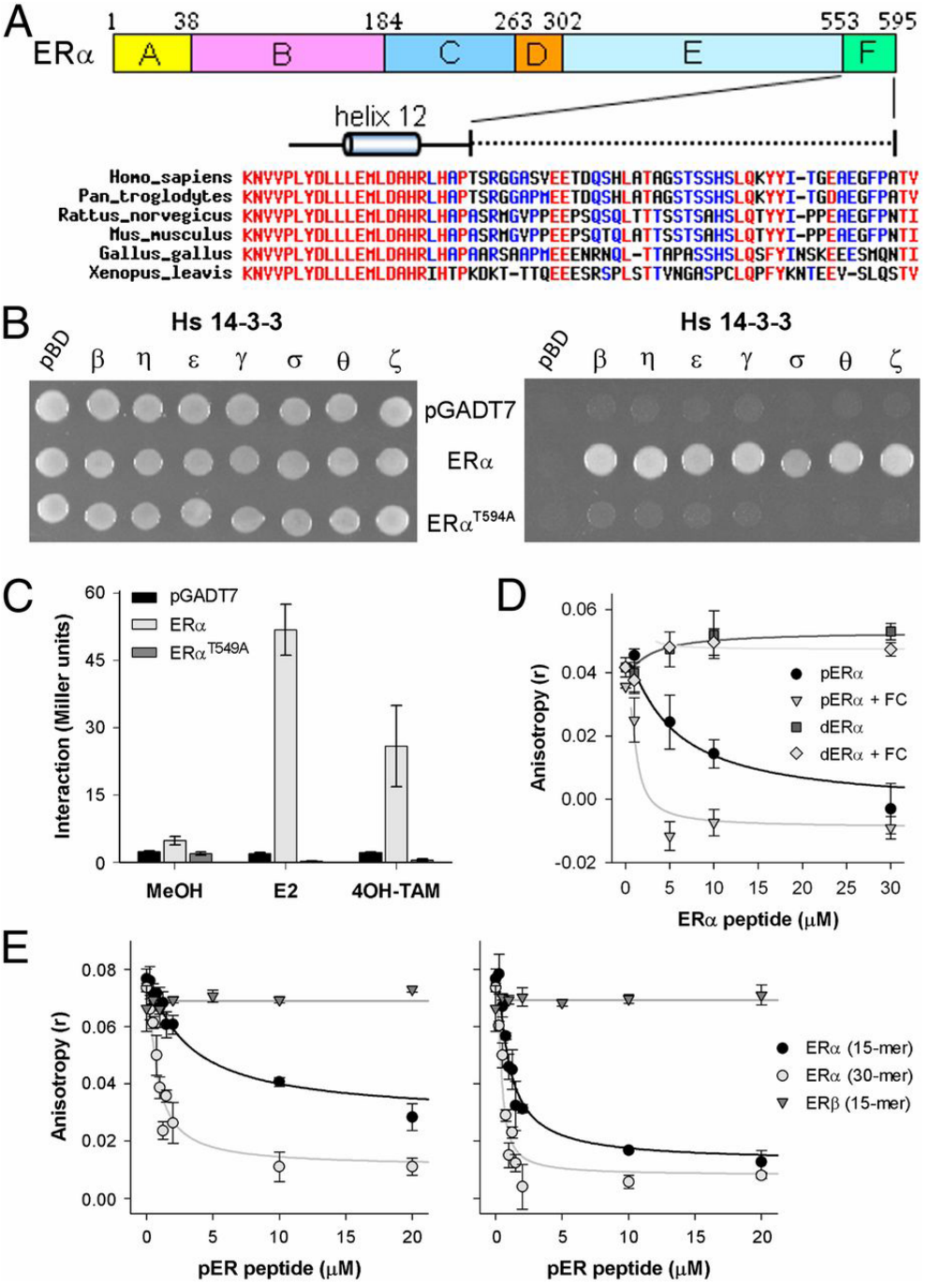
A
ERα
1
38
184
263 302
553 595
A
B
C
D
E
F
helix 12
Homo_sapiens KNVVPLYDLLLEMLDAHRLHAPTSRGGASVEETDQSHLATAGSTSSHSLQKYYI-TGEAEGFPATV
Pan_troglodytes KNVVPLYDLLLEMLDAHRLHAPTSRGGAPMEETDQSHLATAGSTSSHSLQKYYI-TGDAEGFPATV
Rattus_norvegicus KNVVPLYDLLLEMLDAHRLHAPASRMGVPPEEPSQSQLTTTSSTSAHSLQTYYI-PPEAEGFPNTI
Mus_musculus KNVVPLYDLLLEMLDAHRLHAPASRMGVPPEEPSQTQLATTSSTSAHSLQTYYI-PPEAEGFPNTI
Gallus_gallus KNVVPLYDLLLEMLDAHRLHAPAARSAAPMEEENRNQL-TTAPASSHSLQSFYINSKEEESMQNTI
Xenopus_leavis KNVVPLYDLLLEMLDAHRIHTPKDKT-TTQEEESRSPLSTTVNGASPCLQPFYKNTEEV-SLQSTV
B
Hs 14-3-3
pBD
β η ε γ σ θ ζ
pGADT7
ERα
ERα T594A
Hs 14-3-3
pBD
β η ε γ σ θ ζ
C
pGADT7
ERα
ERα T549A
Interaction (Miller units)
60
45
30
15
0
MeOH
E2
4OH-TAM
D
Anisotropy (r)
0.06
0.04
0.02
0.00
-0.02
0 5 10 15 20 25 30
ERα peptide (μM)
pERα
pERα + FC
dERα
dERα + FC
E
Anisotropy (r)
0.08
0.06
0.04
0.02
0.00
0 5 10 15 20
pER peptide (μM)
0 5 10 15 20
pER peptide (μM)
ERα (15-mer)
ERα (30-mer)
ERβ (15-mer)

Figure 1*: Interaction of ERα and 14-3-3 depends on T594 phosphorylation and is enhanced by FC.*
(A) Overview of ERα, with the F domain highlighted and the alignment of the ERα/F domain from various species. (B) ERα-LBD and ERα-LBDT594A interaction with all seven human 14-3-3 isoforms in yeast, tested for colony growth (Left; DDO) and for interaction (Right; TDO). ERα-LBD interacts with all seven human 14-3-3 isoforms, whereas no interaction is observed for ERα-LBDT594A. (C) The 14-3-3θ interactions with ERα-LBD and ERα-LBDT594A with ERα ligands (n = 3, ± SD) (Fig. S1 B and C). (D) Interaction between 14-3-3θ and the C-terminal (de)-phospho-ERα peptide, as measured by fluorescence anisotropy, with (open symbols) or without (closed symbols) FC (n = 2, ±SD) (Fig. S1D and Table S1). (E) Comparison of the interaction of 14-3-3ζ with a short (15 aa) or long (30 aa) C-terminal pERα peptide as well as a short (15 aa) C-terminal pERβ peptide with (Right) or without (Left) FC (n = 2, ±SD).

have been obtained with other 14-3-3 isoforms as well as full-length ERα (Fig. S1 B and C), which shows that (ant)agonist binding to the receptor increases the accessibility of the F domain for 14-3-3 interaction. Using a competitive fluorescence anisotropy 14–3-3 assay, we tested if T594 phosphorylation and FC influence the affinity of the ERα F domain for 14-3-3 proteins (27). The ERα F-domain peptide, last 15 amino acids, revealed two aspects of interaction: phosphorylation of T594 is essential for interaction (in support of the Y2H results) and the presence of FC increases the apparent affinity of the peptide 5- to 16-fold, depending on the 14-3-3 isoform used (**Fig. 1D** and Fig. S1D and Table S1). Although the ERβ protein contains a penultimate serine residue that can be phosphorylated, no interaction with 14-3-3 protein is observed for the phosphorylated ERβ F-domain peptide with or without FC, indicating ER isoform specificity (**Fig. 1E**). Furthermore, a longer ERα F domain phosphopeptide (30 amino acids) is still responsive to FC, while having a higher affinity for 14-3-3 proteins, which suggests that the F domain has multiple points of contact with the 14-3-3 protein (**Fig. 1E**).

Crystal Structure of the Trimeric Complex.
The structural basis for the effects described above was elucidated by co-crystallization of the 15-aa F-domain phosphopeptide (pERα), 14-3-3σ and FC. First, the peptide was crystallized with the 14-3-3 protein. Crystals were obtained within 5–7 d and could directly be flash cooled and diffracted to 2.02 Å. The 14-3-3 protein displayed the typical, W-like shaped dimer with both

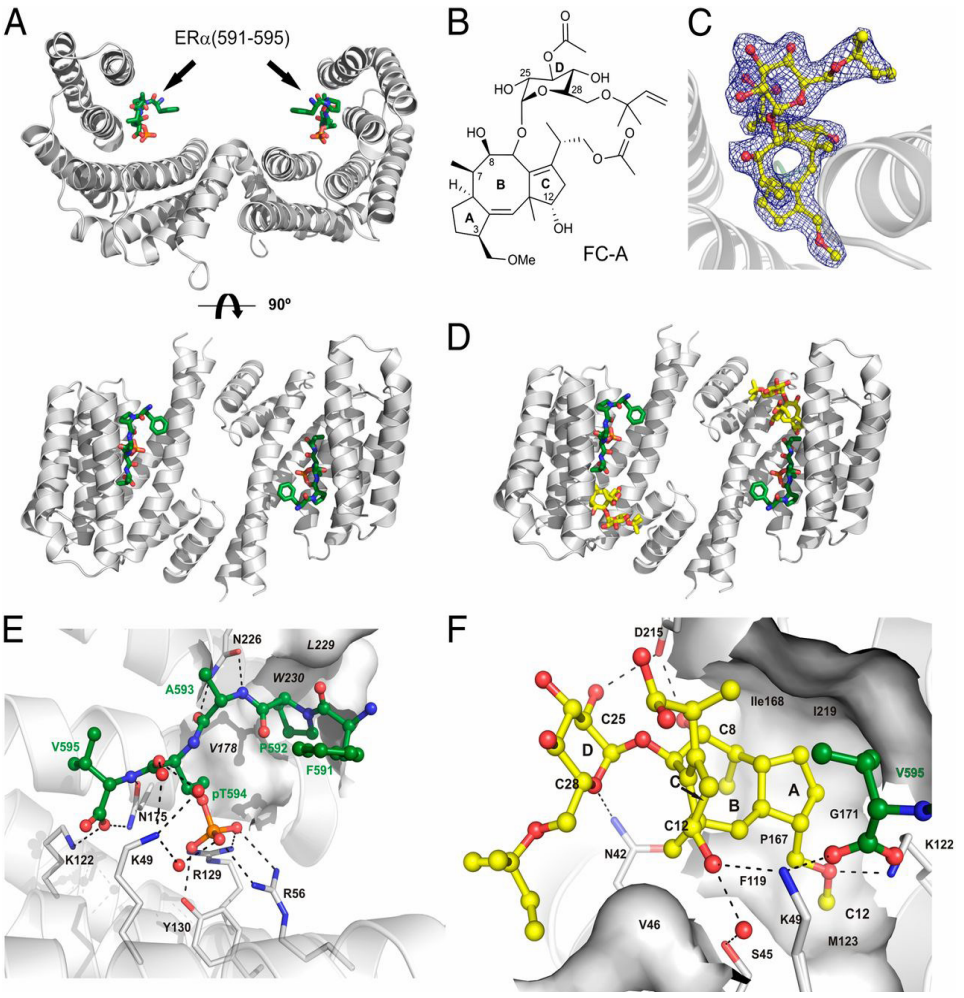

Figure 2: *Cocrystallization of 14-3-3, the phosho-ERα peptide, and fusicoccin. (A) Overview of 14-3-3σ dimer (gray) complexed with phosho-ERα peptide (green). (B)Structure of fusicoccin A (FC). (C) Electron density map (2Fo-Fc, contoured at 1 σ) of fusicoccin (yellow) bound to 14-3-3/pERα complex. (D) Overview of 14-3-3 dimer (gray) complexed with phospho-ERα peptide (green) and FC (yellow). (E) pERα (green) interaction with 14-3-3σ (gray). (F) Fusicoccin (yellow) interaction with 14-3-3σ (gray) and pERα peptide (green). Polar interactions: dashed lines, 14-3-3 residues for interaction, black; hydrophobic 14-3-3 interaction surfaces, white; and water molecules conferring polar interactions, red.*

monomers accommodating one ERα peptide (**Fig. 2A** and Fig. S2A). The peptide shows an elongated conformation and is mainly bound by polar contacts with coordination of the phosphate moiety of pT594 by 14-3-3′s K49, R56, R129 and Y130. To determine how FC (**Fig. 2B**) acts on this protein complex, we soaked binary 14-3-3σ/pERα crystals with FC. Clear additional electron density for the FC molecule could be determined (**Fig. 2C**), allowing the unambiguous spatial determination of the binding mode. One FC molecule is coordinated by each 14-3-3 monomer sitting right next to the C terminus of the pERα peptide (**Fig. 2D** and Fig. S2B). Here, FC is contacting both protein partners thereby filling a gap in the interface of 14-3-3 and pERα (**Fig. 2 E and F** and Fig. S2C). Binding of FC to the binary 14-3-3σ/pERα complex seems to be mainly driven by entropic effects and shape complementarity. FC covers 147.1 Å2 of solvent-exposed surface in the complex and dislocates at least 19 water molecules. Because the free, protein-unbound form of FC (28) is very similar to the structure of FC observed in our ternary complex, also the entropy penalty upon binding of FC is expected to be rather low (see also Table S2).

ERα C Terminus Controls Receptor Dimerization.

To examine the capacity of FC to bind endogenous 14-3-3 and ERα, an affinity pull-down with FC beads (FC was coupled covalently to magnetic hydrazide beads after changing the vinyl group into a reactive aldehyde) was performed in a lysate prepared from MCF-7 cells. The FC beads were first functionally tested (Fig. S3 A and B). Subsequently, a pull-down with MCF-7 cell lysate was performed and this shows that both endogenous 14-3-3 and ERα bind specifically to the FC beads (**Fig. 3A**). In a reverse pull-down experiment with recombinant ERα-LBD as bait, FC also enhanced the binding of 14-3-3 proteins to ERα (**Fig. 3B**). Next, we addressed the question how 14-3-3 protein interaction affects ERα function. In view of the reported function of the F domain in receptor dimerization (16), we tested whether 14-3-3 binding and FC interfere with receptor dimerization. A Y2H β-gal assay with ERα-LBD or ERα-LBDT594A confirmed that the F-domain C terminus controls receptor dimerization (**Fig. 3C**), as reported before (17). Strikingly, the T594A mutation, which annihilates the 14-3-3 interaction (**Fig. 1 B and C**), strongly enhances (ant)agonist-driven receptor dimerization. Similar results have been obtained with full-length ERα or ERαT594A (Fig. S3C). To test whether FC affects ERα dimerization in human cells as well, two N-terminally tagged ERα constructs, HA-ERα and GFP-ERα, were expressed in

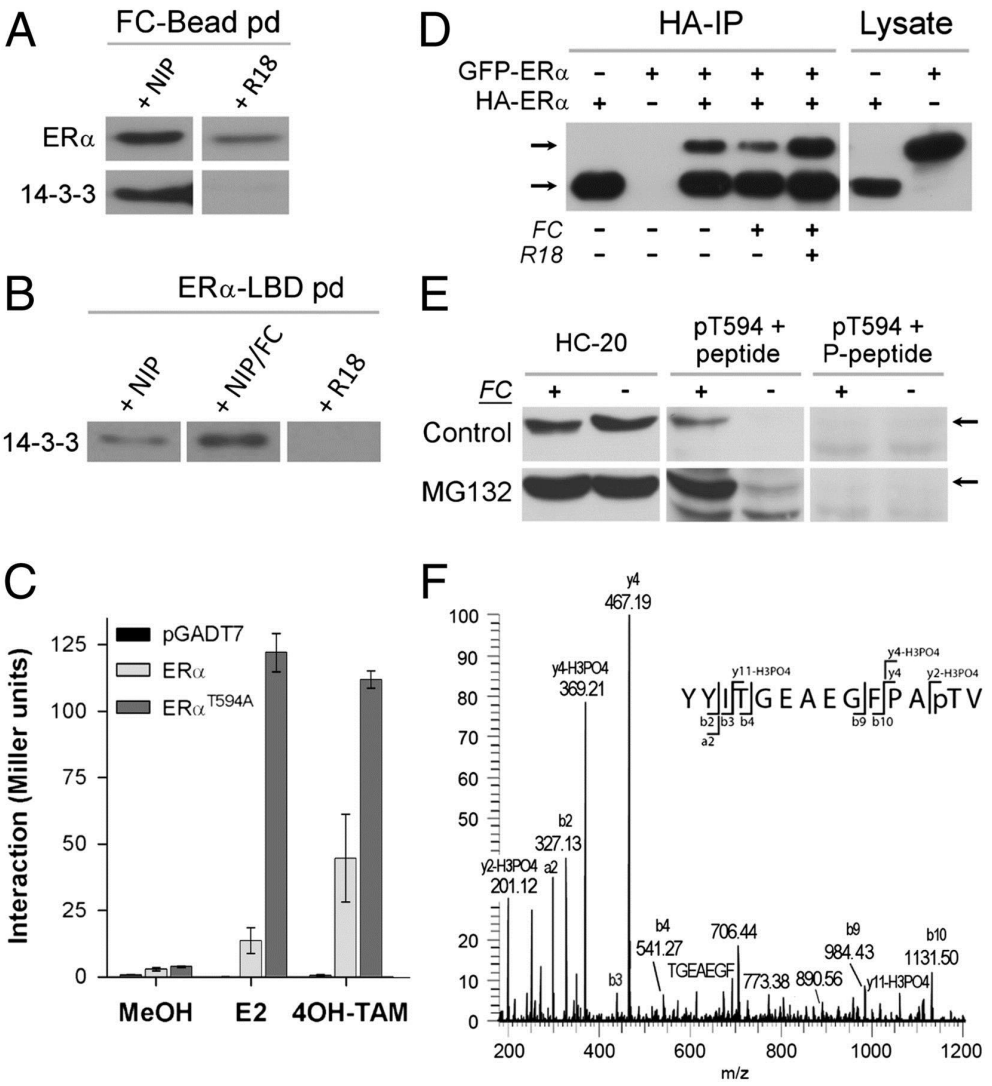

Fig. 3*: 14-3-3 Interaction with ERα affects ERα dimerization and T594 is phosphorylated in MCF-7 cells.*

(A) Pull-down with FC-coated beads isolates endogenous ERα and 14-3-3 (Western blot) from MCF-7 cell lysate; NIP, noninteracting peptide; R18, 14-3-3 blocking peptide (see also Fig. S3 A and B). (B) Endogenous 14-3-3 binding to recombinant ERα-LBD in the presence of NIP, NIP+FC, and R18. (C) Yeast two-hybrid assay with ERα-LBD/ERα-LBD, and ERα-LBDT594A/ERα-LBDT594A showing enhanced dimerization of the ERα mutant (E2, 17β-estradiol; 4OH-TAM, tamoxifen (n

= 3, ±SD) (Fig. S3C). (D) Western blot analysis (HC-20 antibody) of HA-ERα IP from HEK293 cells expressing HA-ERα and GFP-ERα; cells treated with FC (10 μM) show reduced dimerization, whereas R18 added to the cell lysate enhances the dimerization. (E) Western blot analysis with the HC-20 and pT594 antibodies of cell lysate from MCF-7 cells treated with combinations of the proteasome inhibitor MG132 (5 μM) and/or FC (30 μM). The pT594 antibody was used in the presence of the nonphosphorylated (Center) and the T594 phosphorylated ERα peptide (Right).(F) Mass-spectrometry analysis of the C-terminal ERα peptide purified from a trypsin digested MCF-7 cells lysate with the pT594 antibody. Shown is the tandem MS (MS2) spectrum of the C-terminal ERα tryptic peptide showing modification by phosphorylation at threonine 594 (Fig. S5).

HEK293 cells. Immunoprecipitation (IP) of HA-ERα shows receptor dimerization: besides HA-ERα also GFP-ERα is present in the IP (**Fig. 3D**, lane 3). Cells treated with FC show less GFP-ERα in the IP, whereas inclusion of the 14-3-3 competing R18 peptide in the cell lysate during the IP strongly enhances dimerization. These results are in line with the Y2H results and suggest that interaction of 14-3-3 proteins at the ERα C terminus has a negative effect on receptor dimerization.

T594 Is a Distinct ERα Phosphosite.

Thus far, experimental evidence for ERα-T594 phosphorylation has not been described in the literature. However, all evidence shown above indicates that T594 phosphorylation is essential for creating a high-affinity 14-3-3 binding site at the ERα C terminus. To demonstrate endogenous ERα-T594 phosphorylation, we generated an antibody that specifically recognizes the phosphorylated T594 residue. Specificity of the pT594 antibody is demonstrated with a dot blot (Fig. S4A) and Western blotting of cell lysate of HEK293 cells expressing ERα, ERα-T594A, and ERα-Δ4 (Fig. S4B). Next, we did Western blots using the ERα common antibody (HC-20) and the pT594 antibody on cell lysate from MCF-7 cells that were treated without or with FC for 24 h (**Fig. 3E**). Whereas control cells do not show a band recognized by the pT594 antibody, cells treated with FC clearly show a band, which disappears when the antibody is blocked with its antigen, the pT594 peptide. When cells are also treated with the proteasome inhibitor MG132, phosphorylated ERα is already detectable without FC treatment (**Fig. 3E**) and with FC the effect on T594 phosphorylation is even more prominent. To confirm that T594 is a genuine phosphoresidue, we digested the FC/MG132 MCF-7 cell lysate

with trypsin and used the pT594 antibody to IP the C-terminal ERα phosphopeptide. Mass-spectrometry analysis of this fraction identified the C-terminal ERα peptide (14 aa) with T594 phosphorylated (**Fig. 3F** and Fig. S5). We conclude that T594 is a phosphorylated residue in MCF-7 cells and that FC "protects" the T594 phosphosite resulting in increased phosphorylation.

FC Reduces Genome-Wide Chromatin Interactions of ERα.

Because ERα interacts with DNA as a dimer, we expected that an FC/14-3-3-induced reduction of receptor dimerization would prevent ERα/DNA interactions. Chromatin immunoprecipitation (ChIP) was performed for ERα, and the receptor/chromatin interaction for two well-described ERα binding events [nuclear receptor-interacting protein 1 (NRIP1) and X-box binding protein 1 (XBP1)] (29) was studied. For both ERα binding sites, FC significantly reduced the chromatin interaction of ERα as well as its coactivator amplified in breast cancer 1 (AIB1) (**Fig. 4A**). To assess the effect of FC on ERα/chromatin associations on a genome-wide scale, ChIP was followed by high-throughput sequencing (ChIP-seq). Again, FC decreased ERα/chromatin interactions, and peak intensities were decreased by FC treatment (**Fig. 4B**). Under control conditions, 26,987 ERα binding events were found on a genome-wide scale (**Fig. 4C**). This number of binding events was greatly diminished by FC treatment, where 16,829 ERα sites were found. The sites shared under both control and FC conditions ("shared regions") were the strongest ERα binding events, which were significantly lowered in intensity by FC treatment (**Fig. 4D** and quantified in **Fig. 4E**). The less strong ERα binding sites were unique for the control conditions ("control unique") and lost due to an FC-induced decrease of peak intensity beyond the detection threshold of the peak-calling algorithm. Consequently, the number of ERα peaks decreased upon FC treatment (**Fig. 4C**). No selectivity was observed for the type of ERα interaction that was lost (monomer versus dimer) based on DNA motif analysis or whether they were mediated by direct ERα/DNA binding or through specificity protein 1 (SP1) or complexes of the transcription factors Fos and Jun (Fos/Jun) (Fig. S6). These results show that FC-mediated loss of ERα/chromatin interaction is highly effective, nonselective for the mode of ERα chromatin interactions as based on DNA motif analysis, and occurs genome-wide.

Fusicoccin Reduces ERα Transactivation and Cell Growth.

Next, the biological consequences of FC-induced ERα/14-3-3 stabilization and reduced ERα/chromatin interactions were investigated. First, the influ-

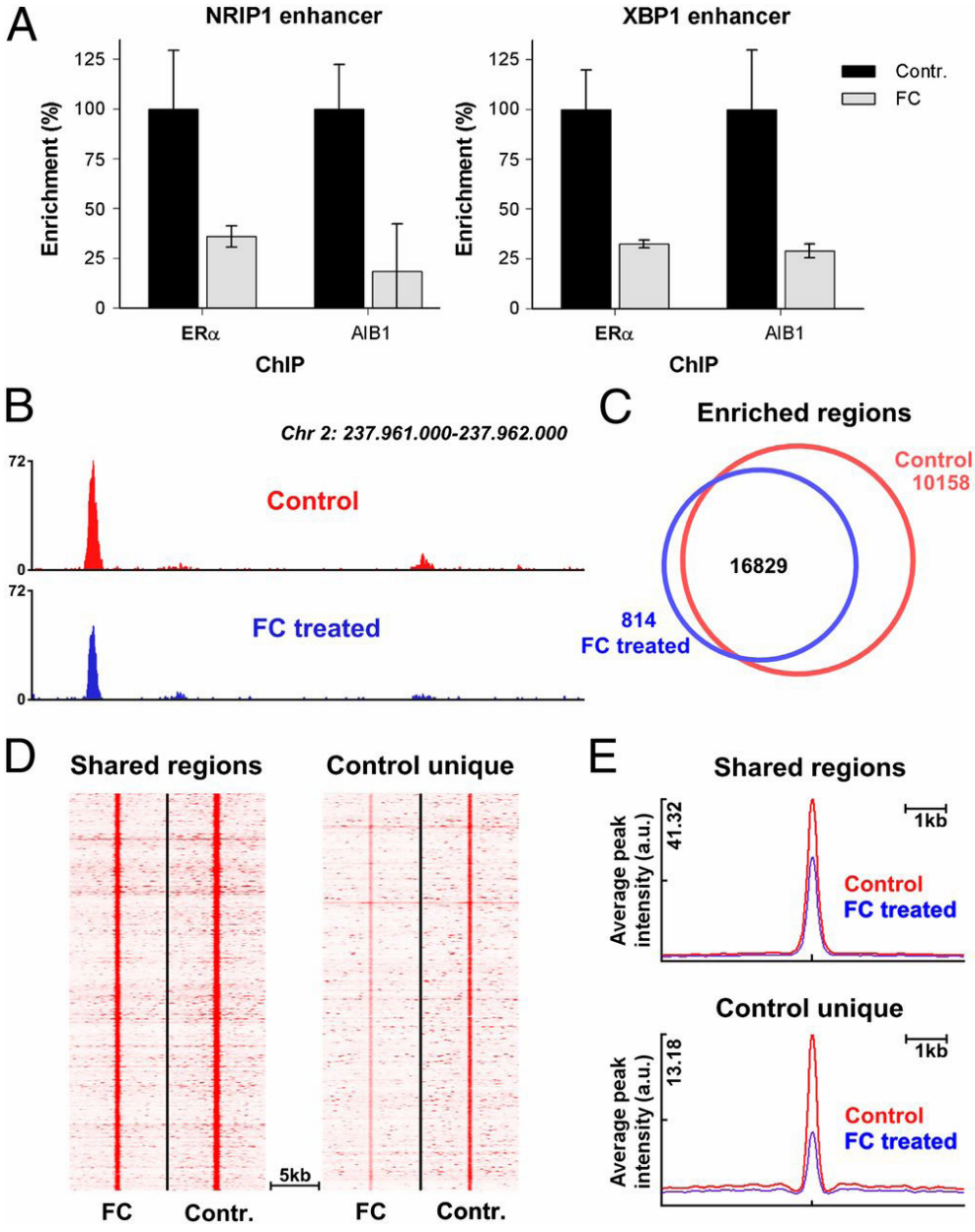

Fig. 4*: FC reduces genome-wide chromatin/ERα interactions.*
(A) qPCR of NRIP1 and XBP1 enhancer elements after ChIP for ERα and AIB1 in the absence or presence of 10 μM FC (n = 3, ±SD). (B) Genome browser snapshot, illustrating decrease of ERα/chromatin interaction after FC treatment. Genomic

coordinates and tag count are indicated. (C) Venn diagram showing ERα binding events in absence (red) and presence (blue) of FC. (D) Heatmap visualizing intensity of ERα binding events in FC and control-treated cells at regions found under both conditions (shared; Left) and sites that are lost after FC treatment (control unique; Right) (E) Average peak intensity of ERα binding sites as visualized in D.

ence of FC on ERα transcriptional activity was tested, as well as the role of the F-domain C-terminal tip therein. To rule out any influence of endogenous receptor, we made use of ERα-negative human osteosarcoma cell line U2OS, a well-annotated model system for ERα action (30). ERα-mediated estrogen response element-luciferase reporter (ERE-luc) expression was measured in U2OS cells cotransfected with ERα wild type (ERα-WT) and two C-terminal mutants: ERα-T594A and ERα-Δ4, a construct lacking the last four amino acids. ERα-T594A may still exhibit partial FC sensitivity, because studies on the FC target in plants (the H+-ATPase) have shown that interaction of the nonphosphorylated H+-ATPase and 14-3-3 proteins do occur, provided that FC is present (31, 32). ERα-Δ4 should be FC insensitive because the amino acids that line the 14-3-3 groove and contact the FC molecule (**Fig. 2**) are missing. As shown in **Fig. 5A**, FC significantly reduces the ERα-WT transcriptional activity in a dose-dependent manner, with an inhibition of more than 60% at 1 nM E2. The transcriptional activity of ERα-Δ4 is indeed unaffected by FC and is much higher than that of ERα-WT (note that the scale of the y axis is different). Cells transfected with ERα-T594A also show enhanced transcriptional activity compared with ERα-WT in the absence of FC and, as expected, the transcriptional activity shows some FC sensitivity, albeit less than that of ERα-WT. These experiments illustrate that the ERα C terminus is essential for regulating ERα activity and for the inhibitory effect of FC thereon. Furthermore, FC does not affect the transcriptional activity of ERβ (**Fig. 5B**), indicating that the 14-3-3/FC interaction is indeed isoform specific (see also Fig. 1E).

To further determine the effect of FC on endogenous ERα-mediated gene transcription, we analyzed transcript levels of a number of E2-dependent genes in the absence and presence of FC. As shown in **Fig. 5C**, FC treatment significantly reduced E2-mediated transcription of these genes. In line with these data, FC treatment significantly inhibited E2-induced cell proliferation in a dose-dependent manner (), and this effect on proliferation was not apoptosis related (Fig. S7).

Cumulatively, we have shown a unique mode of ERα inhibition in-

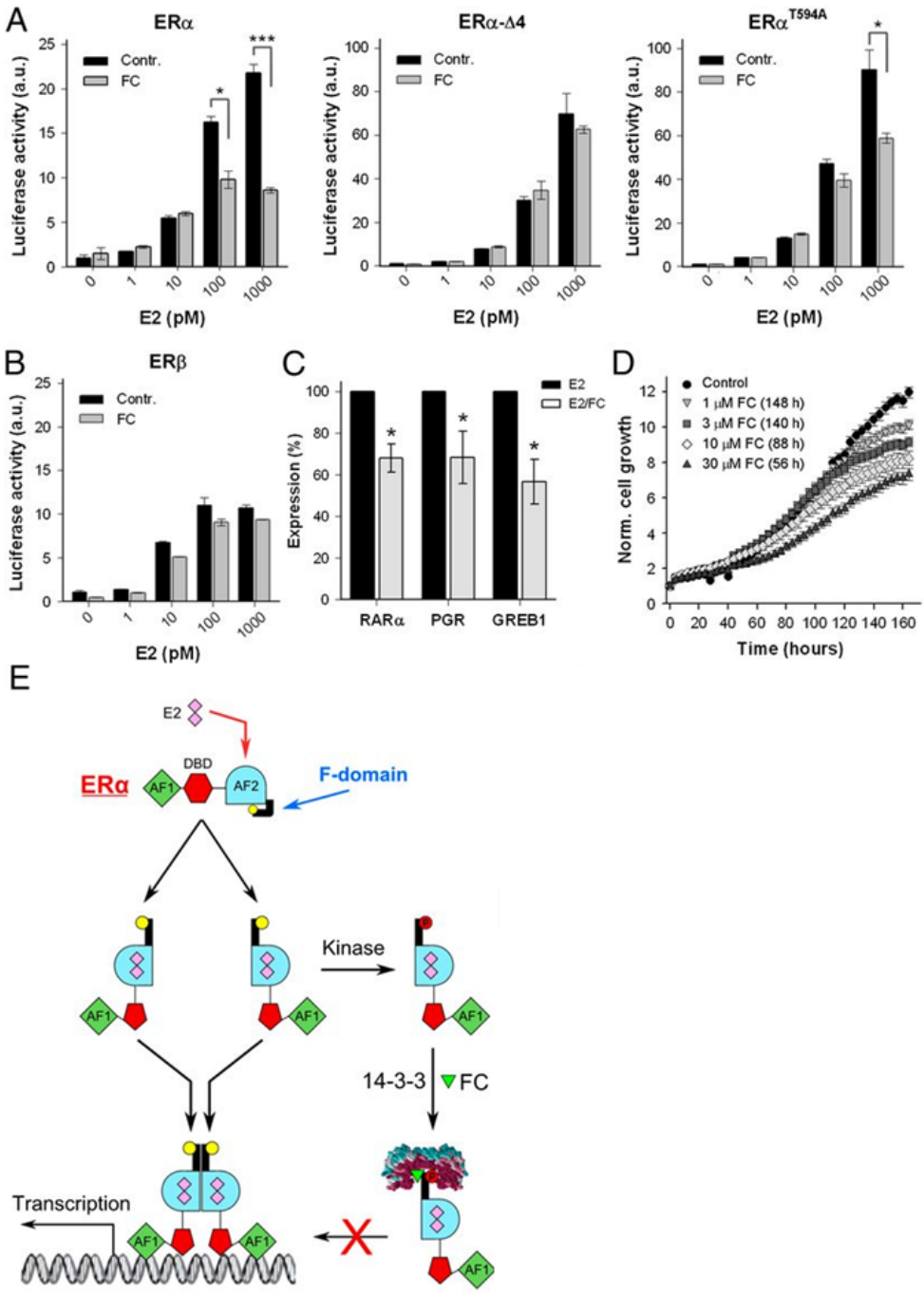
A
ERα
ERα-Δ4
ERα T594A
Contr.
FC
Luciferase activity (a.u.)
E2 (pM)
B
ERβ
C
Expression (%)
E2
E2/FC
RARα
PGR
GREB1
D
Control
1 μM FC (148 h)
3 μM FC (140 h)
10 μM FC (88 h)
30 μM FC (56 h)
Norm. cell growth
Time (hours)
E
E2
DBD
AF1
AF2
ERα
F-domain
Kinase
14-3-3
FC
Transcription

Fig. 5*: Effect of fusicoccin on ERα gene activation and cell growth.*
*(A) Normalized transactivation activity (ERE-luciferase assay) of ERα, ERαΔ4 (lacking the last four amino acids), and ERαT594A, for various E2 concentrations in the presence and absence of 10 μM FC (n = 3, ±SD *P < 0.05; ***P < 0.001). (B) Same as A, now analyzing the normalized ERβ transactivation (n = 2, ±SD). (C) qPCR expression analysis of ERα regulated genes [progesterone receptor (PGR), retinoid acid receptor alpha (RARα), and gene regulated by estrogen in breast cancer 1 (GREB1)] in hormone-deprived MCF-7 cells treated with E2 (10 nM) or E2/FC (10 μM) (n = 7, ±SEM, *P < 0.05). (D) E2-induced MCF-7 cell proliferation is inhibited by FC. Time to reach significant (P < 0.05) inhibition is indicated in parentheses (n = 12, ±SEM) (Fig. S6). (E) Model showing ERα activation, the function of 14-3-3, and FC on the F domain and receptor activation. Ligand binding (E2) drives conformational changes that displace the F domain, which enables receptor dimerization and transcriptional activation. Displacement of the F domain also renders the C-terminal tip (yellow) accessible for phosphorylation of T594 (red). Subsequent 14-3-3 binding, and stabilization by FC, keeps the receptor in a monomeric state, thereby reducing DNA interaction, gene transcription, and cell growth.*

volving the newly identified phosphorylated T594 residue, which operates through the interaction of the ERα F-domain tip with 14-3-3 proteins. Stabilizing this ERα/14-3-3 interaction through small molecule inhibitors like FC suffices in functionally reducing ERα/DNA interactions, gene transcription, and cell proliferation.

Discussion

Blocking ERα functioning is the major treatment modality in luminal breast cancer (33–35). Most efforts to modulate the ERα activity have focused on a single pocket buried in the ERα protein, where agonists, antagonists, and selective modulators interact with ERα: the ligand-binding pocket. Because treatment resistance is commonly observed, focus is shifting toward the identification of small-molecule inhibitors that target sites outside this ligand-binding pocket, like the coactivator-binding groove, allosteric sites in the LBD, and the interface for DNA contact (34, 36). Receptor dimerization is an essential step in the cascade of events through which ERα modulates gene expression and therefore any changes that alter ERα dimerization will have profound effects on ERα function. After binding of ligand, ERα monomers undergo dramatic conformational changes exposing sequences required for dimerization and evidence has been presented that the carboxy terminal

F domain imparts internal restraint on ER dimerization (17, 37). Notably, mutations in the last few amino acids of the F domain somehow relieve the restraint on dimerization imposed by the F domain and enhance transcriptional activity (17). Understanding the molecular mechanism that gives the F-domain C terminus control over ERα dimerization will provide new tools to interfere with the ligand-driven dimerization process and thus ligand-dependent ERα activation in ERα-positive tumor cells.

In this report we demonstrate that the ERα F-domain C terminus contains a mode-III binding motif for 14-3-3 proteins (38) and moreover, that the ERα/14-3-3 interface can be targeted by the small-molecule FC. The effect of FC described here is unique among all known small molecules that modulate the ERα activity, as it targets a unique protein–protein interaction interface and stabilizes rather than disturbs an ERα/macromolecule interaction. This mode of FC action, which can be described as a "molecular glue," has been well documented for the plant ATPase/14-3-3 interaction (21, 22) and this study shows that the compound/substrate interactions, as well as their functional consequences, are conserved across species.

At the molecular level, the Y2H, fluorescence anisotropy and cocrystallization studies all point to an alternative mechanism of ERα regulation, where 14-3-3 proteins interact with the very C terminus of the ERα F domain, with a key role for phosphorylation of the penultimate T594. We uniquely demonstrate that T594 is an in vivo phosphosite in the breast cancer cell line MCF-7. Because phosphorylated ERα accumulates in cells where proteosomal degradation is inhibited, we hypothesize that the T594 phosphorylated ERα is a short-lived intermediate in the cycle of receptor activation/degradation. This may be the reason why phosphorylation of T594 has gone unnoticed thus far. FC clearly enhances the level of T594 phosphorylation, probably because the phosphosite is shielded from phosphatase activity by an increase in affinity for 14-3-3 proteins, a well-known effect described for the FC target in plants, the H+-ATPase (39, 40). This mode-III 14-3-3 interaction provides the framework for a model where the ERα C terminus negatively affects receptor dimerization, consistent with previously published work (17), through interaction with 14-3-3 proteins, as shown here. At the cellular level, the (FC stabilized) interaction between ERα and 14-3-3s negatively affects receptor/DNA interactions, the transactivation activity and ERα-dependent cell growth. Furthermore, this interaction can be targeted by small molecules, like FC, and FC is receptor specific as it only targets ERα without affecting ERβ, which is a positive feature in view of the antiproliferative role described

for ERβ (41, 42).

Taken together, our results establish an alternative and selective mode of ERα regulation (Fig. 5E), where the receptor's F domain becomes amenable for interaction with 14-3-3 proteins after ligand binding. FC is a small molecule ligand that specifically modulates the interaction surface between ERα and its regulatory 14-3-3 protein, albeit at a relatively low affinity. Therefore, this small molecule and related fusicoccanes (43) may provide the very basis for the development of an entirely unique class of antiestrogenic compounds in the treatment of breast cancer.

Materials and Methods

Human ERα (WT or T594A point mutant) and/or 14-3-3 proteins were transfected in yeast cells, using the lithium acetate method (44), to analyze their interaction or study ERα dimerization in a Y2H assay. Double dropout plates (DDOs) were used to check for colony viability and triple dropout plates (TDOs) to test for interaction. The interaction in the presence of various ligands was quantified with a yeast two-hybrid β-galactosidase assay as described before (44).

Competitive anisotropy measurements were performed with ERα peptides consisting of the last 15 (short) or 30 (long) amino acids of ERα, with T594 being phosphorylated (pERα) or dephosphorylated (dERα). In this, the peptides need to compete with the carboxyfluorescein labeled SWpTY peptide (FAM-SWpTY, where pT indicates phosphorylated Threonine) for 14-3-3 binding as described before (27).

In pull-down assays, with GST-ERα-LBD or FC-coated beads, MCF-7 lysate was mixed with a noninteracting peptide (NIP) or the 14-3-3 interacting R18 peptide. The associated endogenous ERα and/or 14-3-3 proteins were subsequently visualized by Western blotting.

ERα activity was measured with an ERE-Luc assay in transfected U2OS cells, using the Dual-Luciferase Reporter Assay (Promega). MCF-7 cell growth and apoptosis induction, treated with FC or methanol and E2, was measured on the IncuCyte FLR (Essen BioScience), using a CellPlayer 96-Well Kinetic Caspase-3/7 apoptosis assay kit. Cell confluence and apoptosis was determined by analyses of phase-contrast/fluorescent images using an algorithm from Confluence v1.5 in combination with IncuCyte software.

For the identification of the phosphorylated C-terminal ERα peptide, cell lysate from MG132/FC-treated MCF-7 cells was trypsin digested and the pT594 antibody was used to IP the phosphopeptide. MS/MS spectra of the

eluted peptides were acquired with a Q Exactive mass spectrometer (ThermoScientific).

ChIPs were performed as described previously (29). Sequences were generated on the Illumina HisEq. 2000 and aligned to the human reference genome. Tools used for enriched region analyses, motif analyses, data snapshots, and heatmap generation are described in SI Materials and Methods. For gene expression analyses equal amounts of cDNA from (un)treated MCF-7 cells were analyzed with SYBR Green (Applied Biosystems) and an MJ Opticon Monitor (BioRad). Data were analyzed with qgene96.

The complex of 14-3-3σΔc (amino acids 1–231) and the short pERα peptide was crystallized using the hanging-drop method. The structure was solved by molecular replacement using Protein Data Bank (PDB) ID: 3P1N as template. The ternary complex was produced by soaking fusicoccin into the binary crystals. Details are described in SI Materials and Methods. The structures of the 14-3-3σΔc/pERα (4JC3) and the 14-3-3σΔc/pERα/FC (4JDD) complexes have been deposited in the PDB.

Acknowledgments

We thank Sjors Kas for his contribution to the anisotropy measurements and Rolf Rose for crystallographic data collection. This study was supported by Nederlandse Organisatie voor Wetenschappelijk Onderzoek (NWO) ECHO Grant 700.54.012. W.Z. is supported by a KWF Dutch Cancer Society Fellowship. Dr. M. Li provided the FAM-SWpTY peptide. D.B. was supported by the DFG grant OT414/2-1.

Author contributions: I.J.D.V.-v.L., K.D.F., R.M., C.O., W.Z., and A.H.d.B. designed research; I.J.D.V.-v.L., D.d.C.P., K.D.F., S.R.P., C.H., D.B., Z.Y., K.A.F., and A.H.d.B. performed research; C.H., R.M., and L.B. contributed new reagents/analytic tools; I.J.D.V.-v.L., D.d.C.P., K.D.F., S.R.P., D.B., Z.Y., K.A.F., C.R.J., T.F.A.d.G., C.O., W.Z., and A.H.d.B. analyzed data; and I.J.D.V.-v.L., T.F.A.d.G., L.B., C.O., W.Z., and A.H.d.B. wrote the paper.

The authors declare no conflict of interest.

References

1. Ariazi EA, Ariazi JL, Cordera F, Jordan VC (2006) Estrogen receptors as therapeutic targets in breast cancer. Curr Top Med Chem 6(3):181–202.

2. Asselin-Labat M-L, et al. (2010) Control of mammary stem cell function by steroid

hormone signalling. Nature 465(7299):798–802.

3. Bergamaschi A, Katzenellenbogen BS (2012) Tamoxifen downregulation of miR-451 increases 14-3-3ζ and promotes breast cancer cell survival and endocrine resistance. Oncogene 31(1):39–47.

4. Zwart W, et al. (2007) PKA-induced resistance to tamoxifen is associated with an altered orientation of ERalpha towards co-activator SRC-1. EMBO J 26(15):3534–3544.

5. Shanle EK, Xu W (2010) Selectively targeting estrogen receptors for cancer treatment. Adv Drug Deliv Rev 62(13):1265–1276.

6. Wardell SE, Marks JR, McDonnell DP (2011) The turnover of estrogen receptor α by the selective estrogen receptor degrader (SERD) fulvestrant is a saturable process that is not required for antagonist efficacy. Biochem Pharmacol 82(2):122–130.

7. Carraz M, Zwart W, Phan T, Michalides R, Brunsveld L (2009) Perturbation of estrogen receptor alpha localization with synthetic nona-arginine LXXLL-peptide coactivator binding inhibitors. Chem Biol 16(7):702–711.

8. Powell E, Wang Y, Shapiro DJ, Xu W (2010) Differential requirements of Hsp90 and DNA for the formation of estrogen receptor homodimers and heterodimers. J Biol Chem 285(21):16125–16134.

9. Zhang YH, Li ZG, Sacks DB, Ames JB (2012) Structural basis for Ca2+-induced activation and dimerization of estrogen receptor α by calmodulin. J Biol Chem 287(12):9336–9344.

10. Brzozowski AM, et al. (1997) Molecular basis of agonism and antagonism in the oestrogen receptor. Nature 389(6652):753–758.

11. Mahalingam D, et al. (2009) Targeting HSP90 for cancer therapy. Br J Cancer 100(10):1523–1529.

12. Fliss AE, Benzeno S, Rao J, Caplan AJ (2000) Control of estrogen receptor ligand binding by Hsp90. J Steroid Biochem Mol Biol 72(5):223–230.

13. Helsen C, et al. (2012) Structural basis for nuclear hormone receptor DNA binding. Mol Cell Endocrinol 348(2):411–417.

14. Powell E, Xu W (2008) Intermolecular interactions identify ligand-selective activity of estrogen receptor alpha/beta dimers. Proc Natl Acad Sci USA 105(48):19012–19017.

15. Peters GA, Khan SA (1999) Estrogen receptor domains E and F: Role in dimerization and interaction with coactivator RIP-140. Mol Endocrinol 13(2):286–296.

16. Skafar DF, Zhao CQ (2008) The multifunctional estrogen receptor-alpha F domain. Endocrine 33(1):1–8.

17. Yang J, Singleton DW, Shaughnessy EA, Khan SA (2008) The F-domain of estrogen receptor alpha inhibits ligand induced receptor dimerization. Mol Cell Endocrinol 295(1-2):94–100.

18. Ballio A, et al. (1964) Fusicoccin: A New Wilting Toxin produced by Fusicoccum

amygdali Del. Nature 203(4942):297.

19. de Vries-van Leeuwen IJ, et al. (2010) Fusicoccin-A selectively induces apoptosis in tumor cells after interferon-alpha priming. Cancer Lett 293(2):198–206.

20. Korthout HA, de Boer AH (1994) A fusicoccin binding protein belongs to the family of 14-3-3 brain protein homologs. Plant Cell 6(11):1681–1692.

21. Würtele M, Jelich-Ottmann C, Wittinghofer A, Oecking C (2003) Structural view of a fungal toxin acting on a 14-3-3 regulatory complex. EMBO J 22(5):987–994.

22. Ottmann C, et al. (2007) Structure of a 14-3-3 coordinated hexamer of the plant plasma membrane H+ -ATPase by combining X-ray crystallography and electron cryomicroscopy. Mol Cell 25(3):427–440.

23. Morrison DK (2009) The 14-3-3 proteins: Integrators of diverse signaling cues that impact cell fate and cancer development. Trends Cell Biol 19(1):16–23.

24. Steinacker P, Aitken A, Otto M (2011) 14-3-3 proteins in neurodegeneration. Semin Cell Dev Biol 22(7):696–704.

25. Jahn T, et al. (1997) The 14-3-3 protein interacts directly with the C-terminal region of the plant plasma membrane H(+)-ATPase. Plant Cell 9(10):1805–1814.

26. Tanenbaum DM, Wang Y, Williams SP, Sigler PB (1998) Crystallographic comparison of the estrogen and progesterone receptor's ligand binding domains. Proc Natl Acad Sci USA 95(11):5998–6003.

27. Wu M, et al. (2006) SWTY—a general peptide probe for homogeneous solution binding assay of 14-3-3 proteins. Anal Biochem 349(2):186–196.

28. Ballio A, et al. (1991) H-1-NMR conformational study of Fusicoccin and related compounds - molecular conformation and biological activity. Phytochemistry 30(1):137–146.

29. Zwart W, et al. (2011) Oestrogen receptor-co-factor-chromatin specificity in the transcriptional regulation of breast cancer. EMBO J 30(23):4764–4776.

30. Kallio A, et al. (2008) Estrogen and the selective estrogen receptor modulator (SERM) protection against cell death in estrogen receptor alpha and beta expressing U2OS cells. Mol Cell Endocrinol 289(1-2):38–48.

31. Fuglsang AT, et al. (2003) The binding site for regulatory 14-3-3 protein in plant plasma membrane H+-ATPase: involvement of a region promoting phosphorylation independent interaction in addition to the phosphorylation-dependent C-terminal end. J Biol Chem 278(43):42266–42272.

32. Jelich-Ottmann C, Weiler EW, Oecking C (2001) Binding of regulatory 14-3-3 proteins to the C terminus of the plant plasma membrane H+ -ATPpase involves part of its autoinhibitory region. J Biol Chem 276(43):39852–39857.

33. Zwart W, Theodorou V, Carroll JS (2011) Estrogen receptor-positive breast cancer: A multidisciplinary challenge. Wiley Interdiscip Rev Syst Biol Med 3(2):216–230.

34. Shapiro DJ, Mao C, Cherian MT (2011) Small molecule inhibitors as probes for estrogen and androgen receptor action. J Biol Chem 286(6):4043–4048.

35. Nilsson S, Koehler KF, Gustafsson JA (2011) Development of subtype-selective oestrogen receptor-based therapeutics. Nat Rev Drug Discov 10(10):778–792.

36. Moore TW, Mayne CG, Katzenellenbogen JA (2010) Minireview: Not picking pockets: Nuclear receptor alternate-site modulators (NRAMs). Mol Endocrinol 24(4):683–695.

37. Koide A, et al. (2007) Identification of regions within the F domain of the human estrogen receptor alpha that are important for modulating transactivation and protein-protein interactions. Mol Endocrinol 21(4):829–842.

38. de Boer AH, van Kleeff PJ, Gao J (2013) Plant 14-3-3 proteins as spiders in a web of phosphorylation. Protoplasma 250(2):425–440.

39. Olsson A, Svennelid F, Ek B, Sommarin M, Larsson C (1998) A phosphothreonine residue at the C-terminal end of the plasma membrane H+-ATPase is protected by fusicoccin-induced 14-3-3 binding. Plant Physiol 118(2):551–555.

40. Kinoshita T, Shimazaki K (2001) Analysis of the phosphorylation level in guard-cell plasma membrane H+-ATPase in response to fusicoccin. Plant Cell Physiol 42(4):424–432.

41. Bartella V, et al. (2012) Estrogen receptor beta binds Sp1 and recruits a corepressor complex to the estrogen receptor alpha gene promoter. Breast Cancer Res Treat 134(2):569–581.

42. Fox EM, Davis RJ, Shupnik MA (2008) ERbeta in breast cancer—onlooker, passive player, or active protector? Steroids 73(11):1039–1051.

43. de Boer AH, de Vries-van Leeuwen IJ (2012) Fusicoccanes: Diterpenes with surprising biological functions. Trends Plant Sci 17(6):360–368.

44. Schoonheim PJ, et al. (2007) 14-3-3 adaptor proteins are intermediates in ABA signal transduction during barley seed germination. Plant J 49(2):289–301.

Supplementary information

Fig. S1. *C-terminal ERα F domain tip interacts with 14-3-3 proteins.*
(A) Alignment of the last 52 amino acids of human ERα and the H+-ATPase of Nicotiana plumbaginifolia (PMA2) and Arabidopsis thaliana (AHA2). The three amino acids most important for the FC/14-3-3/receptor complex formation are indicated (↓). (B) Yeast two-hybrid assay; ligands stimulate the interaction of various 14-3-3 isoforms with WT ERα-LBD, but not ERα-LBDT594A. (C) Quantification of the interaction of 14-3-3θ with full-length WT ERα and ERαT594A, in the presence of ERα ligands. (D) Analysis of the interaction between the short (15 aa) phosphorylated C-terminal ERα peptide (pERα) and all human 14-3-3 isoforms and 14-3-3σ-ΔC. Curves are fitted as described in SI Material and Methods.

Fig. S2. *Cocrystallization of 14-3-3 and the pERα peptide and soaked fusicoccin.*

(A) Stereoview of the pERα peptide (green) in the 2Fo-Fc density map (contoured at 1σ) occupying half of the amphipathic 14-3-3 binding groove (white surface). (B) Stereoview of the pERα peptide (green) and fusicoccin (yellow) in the 2Fo-Fc density map (contoured at 1σ) occupying the amphipathic full binding groove of a 14-3-3σ monomer (white). (C) Detailed view of the interaction of ERα (green) and fusicoccin (yellow) with 14-3-3σ (white). Polar interactions are indicated by dashed lines and 14-3-3 residues implicated in these interactions are labeled in black. Hydrophobic 14-3-3 interaction surface is depicted as white solid surface. Red spheres are water molecules conferring polar interactions.

Fig. S3. *Functional test on FC beads and 14-3-3 interaction with full-length ERα affects dimerization.*
(A) Specifically bound endogenous 14-3-3 proteins can only be eluted from FC-coupled beads (FC beads) with the 14-3-3 interacting R18 peptide, when bound in the presence of a C-terminal peptide derived from the plant H+-ATPase (YpTV) and not with a noninteracting peptide (NIP). (B) 14-3-3 Western blot on the pull-down samples of A confirms the specificity of the 14-3-3 interaction to the FC-coupled beads. (C) Yeast two-hybrid assay for ERα dimerization: The full-length-ERα/ERα-LBD and full length-ERαT594A/ERα-LBDT594A dimerize in the presence of ERα ligands.

Fig. S4. *The pT594-antibody is specific for the T594-phosphorylated ERα C-terminal epitope.*
(A) Dot blot with different amounts of nonphosphorylated (peptide: KYYITGEAEGFPATV) and phosphorylated peptide (P-peptide: KYYITGEAEGFPATP V) spotted. The blot was probed with the pT594-ERα antibody. (B) Western blot with HC-20 antibody and pT594-ERα antibody on cell lysate of HEK293 cells expressing wild-type ERα, ERα-T594A, and ERα-Δ4; cells were grown with FC (10 μM) for 24 h. Whereas the HC-20 antibody shows that ERα is expressed in all three transfected cells, the pT594-ERα antibody only recognizes a band in wild-type ERα transfected cells. This demonstrates that the pT594-ERα antibody is specific for the T594 phosphorylated ERα protein.

Fig. S5. *Mass-spectrometry analysis of the C-terminal ERα peptide shows phosphorylation of the penultimate threonine, T594.*
(A) Extracted ion chromatogram of synthetic ERα C-terminal tryptic phosphopeptide YYITGEAEGFPApTV phosphorylated at T594. The extraction window is m/z 799.31–38. (B) The corresponding peptide from MCF-7 digest, after IP is shown. In A and B coelution at 89–90 min is observed. (C) Accurate intact mass of the peptide, corresponding to the [M+2H]2+ monoisotopic peak at m/z 799.3447, for the synthetic and MCF7-derived phosphopeptide, respectively. (D) See C. (E) MS/MS spectrum of synthetic YYITGEAEGFPApTV. The absence of basic residues (protein C terminus) and presence of acidic residues, as well as a phosphate

group, result in a poor MS/MS spectrum. However, the y2-H3PO4 (m/z 201.1234), y4 (m/z 467.1901), and y4-H3PO4 (m/z 369.2132) ions conclusively localize the phosphate group to T594. (F) Corresponding MS/MS spectrum for the MCF-7–derived phosphopeptide. The fragment ions b2, a2, y2-H3PO4, y4-H3PO4, and y4 ions are detected in similar intensity ratios as observed for the synthetic phosphopeptide identifying the MCF-7–derived phosphopeptide and localizing the site of phosphorylation to T594.

Fig. S6. *ERα/DNA binding mode is not selectively altered by FC treatment.*
(A) Top three motifs for the shared (Left) and control unique (Right) ERα binding events. (B) Average peak intensity of shared (Left) and control unique (Right) ERα binding events mediated directly by ERα or through specificity protein 1 (SP1) and complexes of the transcription factors Fos and Jun (Fos/Jun) as identified through motif scanning of ERα-binding sites, in the absence (red) or presence (blue) of FC.

Fig. S7. *Fusicoccin does not induce apoptosis in E2-treated MCF-7 cells.*
E2-induced MCF-7 apoptosis was assessed over time in the presence of various FC concentrations (30 μM FC shown here), by analyzing the CellPlayer 96-Well Kinetic Caspase-3/7 Apoptosis assay kit. For all FC concentrations, no significant apoptosis induction was observed.

Fig. S1

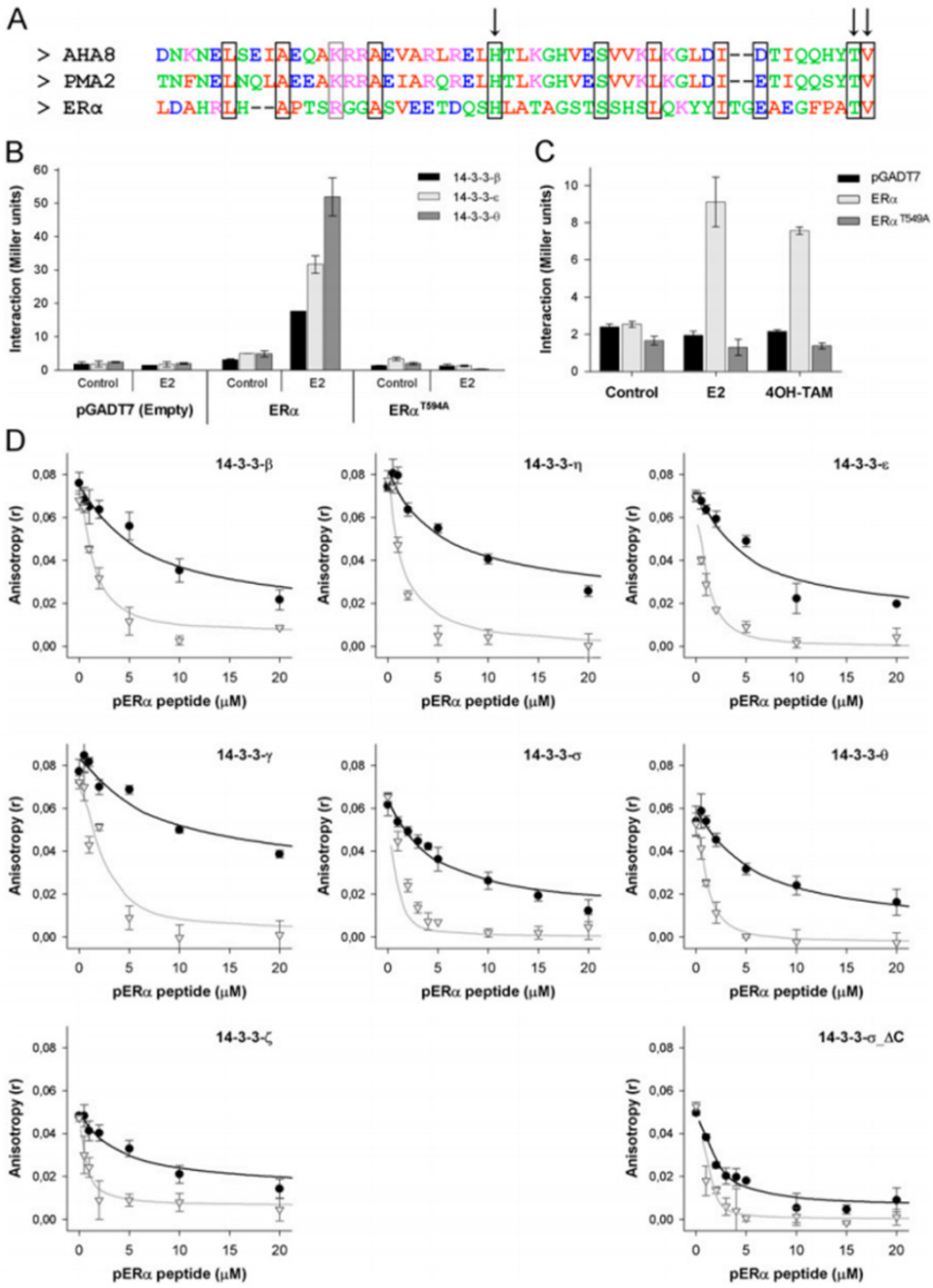
A
> AHA8
> PMA2
> ERα
B
Interaction (Miller units)
14-3-3-β
14-3-3-ε
14-3-3-θ
Control
E2
pGADT7 (Empty)
ERα
ERα T594A
C
Interaction (Miller units)
pGADT7
ERα
ERα T549A
Control
E2
4OH-TAM
D
14-3-3-β
14-3-3-η
14-3-3-ε
14-3-3-γ
14-3-3-σ
14-3-3-θ
14-3-3-ζ
14-3-3-σ_ΔC
Anisotropy (r)
pERα peptide (μM)

Fig. S2

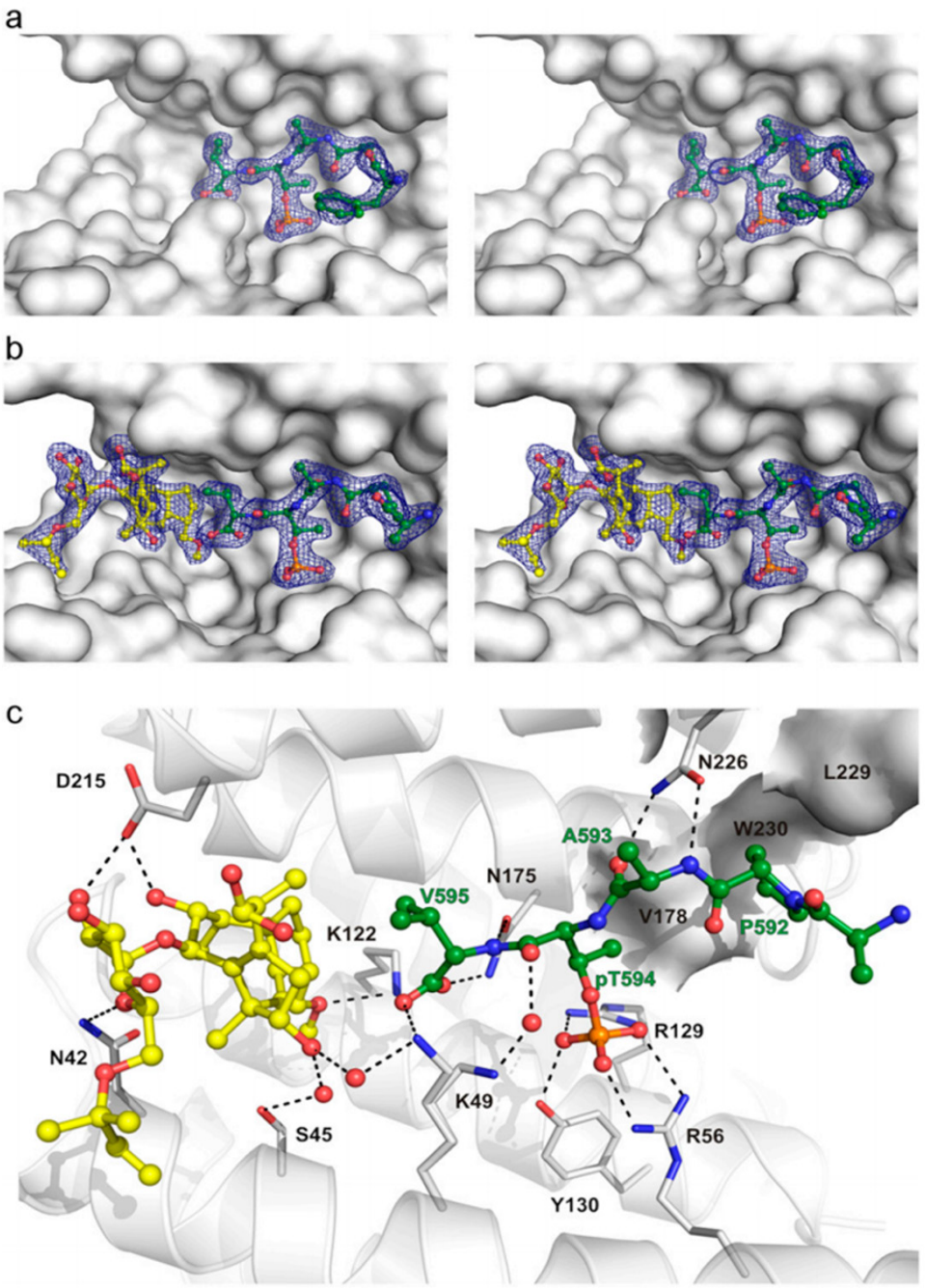
a
b
c
D215
N226
L229
A593
W230
N175
V595
V178
P592
K122
pT594
R129
N42
K49
S45
R56
Y130

Fig. S3

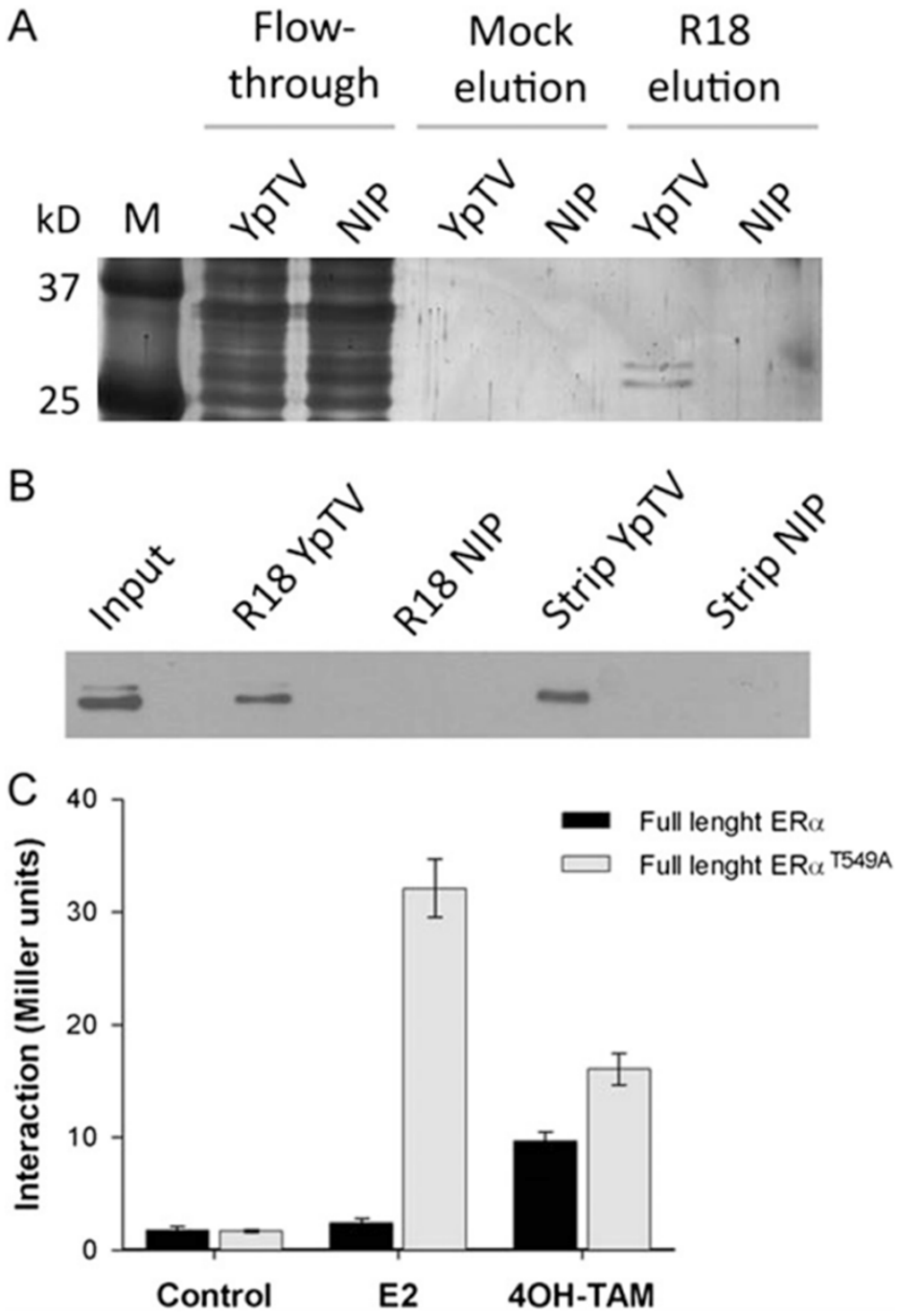
A
Flow-through
Mock elution
R18 elution
kD
M
YpTV
NIP
YpTV
NIP
YpTV
NIP
37
25
B
Input
R18 YpTV
R18 NIP
Strip YpTV
Strip NIP
C
Interaction (Miller units)
40
30
20
10
0
Full lenght ERα
Full lenght ERα T549A
Control
E2
4OH-TAM

Fig. S4

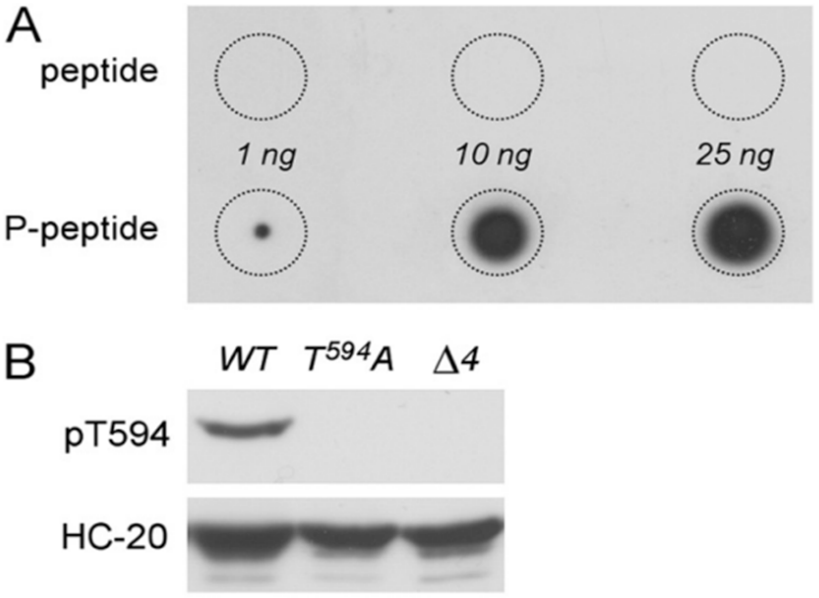
A
peptide
1 ng
10 ng
25 ng
P-peptide
B
WT
T594A
Δ4
pT594
HC-20

Fig. S5

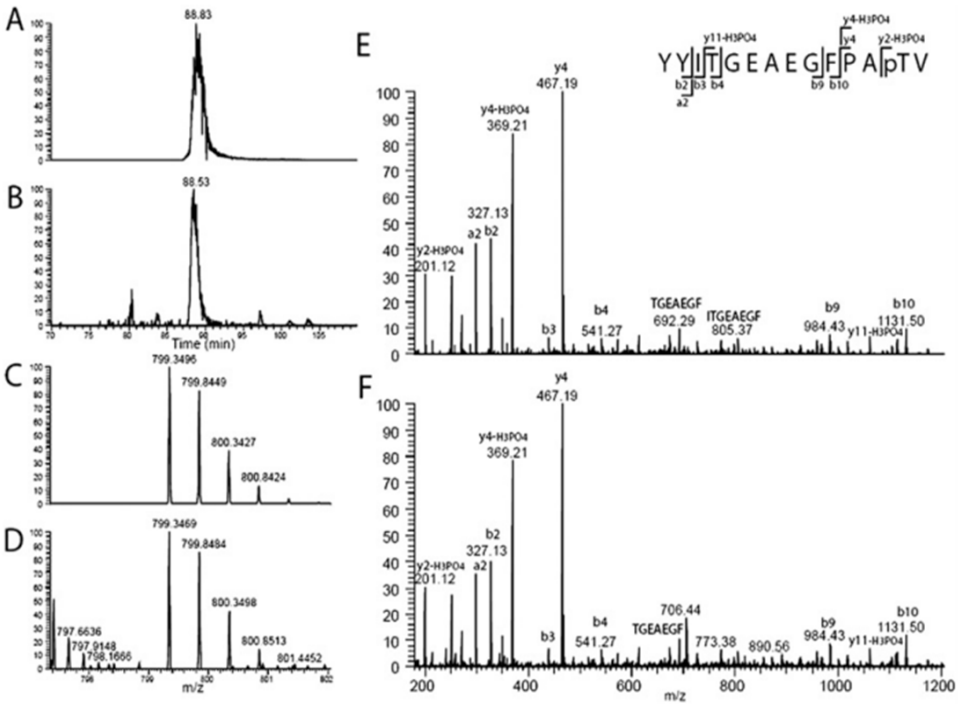
A
88.83
B
88.53
Time (min)
C
799.3496
799.8449
800.3427
800.8424
D
799.3469
799.8484
800.3498
800.8513
797.6636
797.9148
798.1666
801.4452
m/z
E
y4-H3PO4
y11-H3PO4
y4
y2-H3PO4
YYIITGEAEGFPAPTV
b2 b3 b4
b9 b10
a2
y4
467.19
y4-H3PO4
369.21
327.13
a2 b2
y2-H3PO4
201.12
b4
541.27
TGEAEGF
692.29
ITGEAEGF
805.37
b3
b9
984.43
b10
1131.50
y11-H3PO4
F
y4
467.19
y4-H3PO4
369.21
b2
327.13
a2
y2-H3PO4
201.12
706.44
b4
541.27
TGEAEGF
b3
773.38
890.56
b9
984.43
b10
1131.50
y11-H3PO4
m/z

Fig. S6

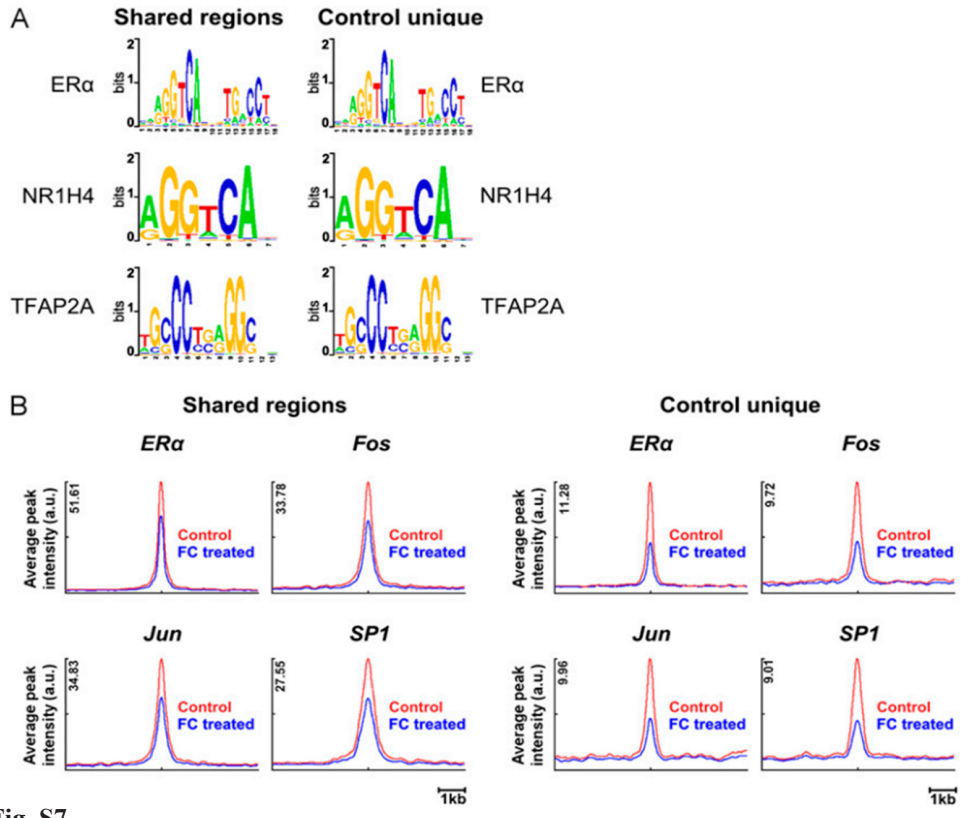
A
Shared regions
Control unique
ERα
NR1H4
TFAP2A
bits
B
Shared regions
Control unique
ERα
Fos
Jun
SP1
Average peak intensity (a.u.)
51.61
33.78
11.28
9.72
34.83
27.55
9.96
9.01
Control
FC treated
1kb

Fig. S7

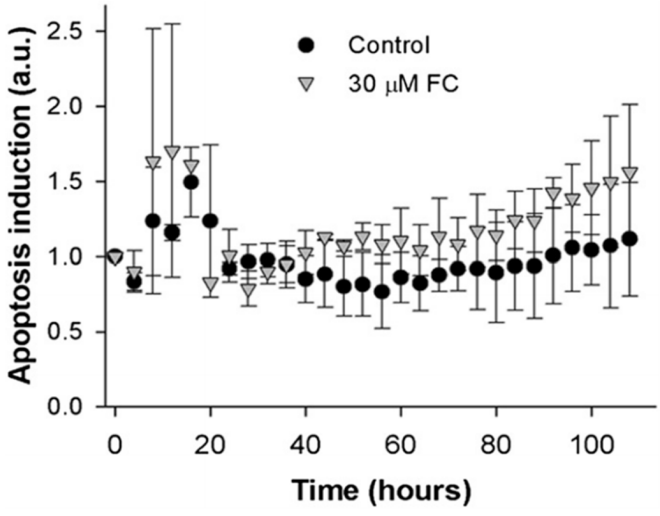
Apoptosis induction (a.u.)
Time (hours)
Control
30 μM FC
0.0
0.5
1.0
1.5
2.0
2.5
0
20
40
60
80
100

Table S1. FC enhances the affinity of the short pERα peptide for all 14-3-3 isoforms

K_d, μM, ±SEM	Control	10 μM FC	Affinity increase
β	0.99 (0.29)	0.11 (0.03)	9.1
η	0.94 (0.32)	0.19 (0.06)	4.9
ε	0.69 (0.21)	0.07 (0.04)	10.4
γ	1.09 (0.36)	0.15 (0.11)	7.1
σ	1.61 (0.32)	0.10 (0.03)	16.4
θ	0.90 (0.20)	0.06 (0.01)	15.1
ζ	0.57 (0.18)	0.05 (0.02)	10.9
σ-ΔC	0.33 (0.07)	0.07 (0.05)	5

Interaction affinity (K_d) of the short pERα peptide for all 14-3-3 isoforms, as calculated from the curves in Fig. S1*D*. Values in parenthesis are +/– SEM.

Table S2. Data collection and refinement statistics for 4JC3 and 4JDD

	4JC3	4JDD
Data collection		
Space group	$C222_1$	$C222_1$
Cell dimensions		
A, b, c, Å	82.2, 112.49, 62.45	82.49, 111.43, 62.24
A, β, γ, °	90, 90, 90	90, 90, 90
Resolution, Å	19.52–2.05 (2.1–2.05)	19.80–2.1 (2.15–2.0)
R_{meas}, %	8.4 (34.9)	12.0 (51.0)
I/σI	24.16 (6.85)	17.79 (4.77)
Completeness, %	99.3	100.0
Redundancy	14.94 (14.7)	15.1 (14.9)
Refinement		
Resolution, Å	19.5–2.05 (2.1–2.05)	19.80–2.1 (2.15–2.0)
No. reflections	141777	135424
Unique reflections	18518	17090
R_{work}/R_{free}	0.1778/0.235	0.1924/0.2316
No. atoms		
Protein	1850	1847
Ligand	42	42 (FUSICOCCIN 48)
Solvent	177	101
B factors, $Å_2$		
Protein	14.3	19.70
Ligand	23.7	26.78 (FUSICOCCIN 23.14)
Water	19.01	21.0
R.m.s. deviations		
Bond lengths, Å	0.019	0.020
Bond angles, °	1.767	1.992
Ramachandran plot		
Favored, %	98.7	97.9
Allowed, %	1.7	2.1
Generously allowed, %	0	0
Disallowed, %	0	0

Values in parenthesis are for the highest resolution shell.